Supplementary information for "Stable Deuterium-Tritium plasmas with improved confinement in the presence of energetic ions instabilities"

Jeronimo Garcia[1], Yevgen Kazakov[2], Rui Coelho[3], Mykola Dreval[4], Elena de la Luna[5], Emilia R. Solano[5], Žiga Štancar[6], Jacobo Varela[7,8], Matteo Baruzzo[9], Emily Belli[10], Phillip J. Bonofiglo[11], Jeff Candy[10], Costanza F. Maggi[6], Joelle Mailloux[6], Samuele Mazzi[1], Jef Ongena[2], Juan R. Ruiz [12], Michal Poradzinski[6], Sergei Sharapov[6], David Zarzoso[13] and JET contributors

[1] *CEA, IRFM, F-13108 Saint-Paul-lez-Durance, France.*
[2] *Laboratory for Plasma Physics, LPP-ERM/KMS, EUROfusion Consortium member, TEC Partner, Brussels, Belgium.*
[3] *Instituto de Plasmas e Fusao Nuclear, Instituto Superior Técnico, Universidade de Lisboa, Lisboa, Portugal.*
[4] *National Science Center Kharkiv Institute of Physics and Technology, 1 Akademichna Str., Kharkiv 61108, Ukraine.*
[5] *Laboratorio Nacional de Fusión, CIEMAT, 28040 Madrid, Spain.*
[6] *United Kingdom Atomic Energy Authority, Culham Campus, Abingdon, OX14 3DB, United Kingdom of Great Britain and Northern Ireland.*
[7] *Universidad Carlos III de Madrid, 28911 Leganes, Madrid, Spain.*
[8] *Institute for Fusion Studies, Department of Physics, University of Texas at Austin, Austin, Texas 78712, USA.*
[9] *Dip.to Fusione e Tecnologie per la Sicurezza Nucleare, ENEA C. R. Frascati, via E. Fermi 45, 00044 Frascati (Roma), Italy.*
[10] *General Atomics, PO Box 85608, San Diego, CA 92186-5608, United States of America.*
[11] *Princeton Plasma Physics Laboratory, Princeton, New Jersey 08540, USA.*
[12] *Rudolf Peierls Centre for Theoretical Physics,University of Oxford,Oxford OX1 3NP,United Kingdom.*
[13] *Aix Marseille Univ, CNRS, Centrale Med, M2P2, Marseille, France.*

Supplementary Note 1. Global characteristics of the discharges #99896 and #99817

Supplementary Table 1: Summary of the main parameters for the discharges #99896 and #99817. I_p is the toroidal current, B_T is the toroidal magnetic field, q_{95} is the safety factor at 95% of the poloidal flux, κ is the triangularity, δ is the elongation, β_N is the normalized β, $H_{98}(y,2)$ is the ratio between the thermal energy confinement time over the IPB98(y,2) scaling, P_{aux} is the total NBI+ICRF injected power, P_{fus} is the maximum power produced by D-T fusion reactions, f_{Gr} is the Greenwald fraction, n_T/n is the ratio of the Tritium density over the total ion density.

Discharge	I_p [MA]	B_T [T]	q_{95}	κ/δ	β_N	$H_{98}(y,2)$	P_{aux} [MW]	P_{fus} [MW]	f_{Gr}	n_T/n[%]
#99896	1.9	2.75	4.5	0.29/1.67	1.2	1.0	8.0	0.5	0.45	40
#99817	2.0	3.70	5.9	0.28/1.65	0.9	0.8	7.5	1.0	0.42	85

Supplementary Note 2. Detailed characteristics of the discharge #99817

The main characteristics of the discharge #99817, with 85% of T concentration, are shown in Supplementary Fig. 1. Compared to the discharge #99896, the same magnetic perturbation pattern is seen as shown in Supplementary Fig. 1. However, due to the higher B_T and lower beta, the intensity of the TAE perturbations is lower, and both faint TAE modes and marginally stable modes, detected by the Alfvén eigenmode active diagnostic (AEAD) [1], coexist.

The total amount of electron heating in the discharge #99817 is $\sim$ 70% as obtained from TRANSP. The electron heating from NBI and ICRF, P_e is higher than the ion heating, P_i, in the whole plasma radius as shown

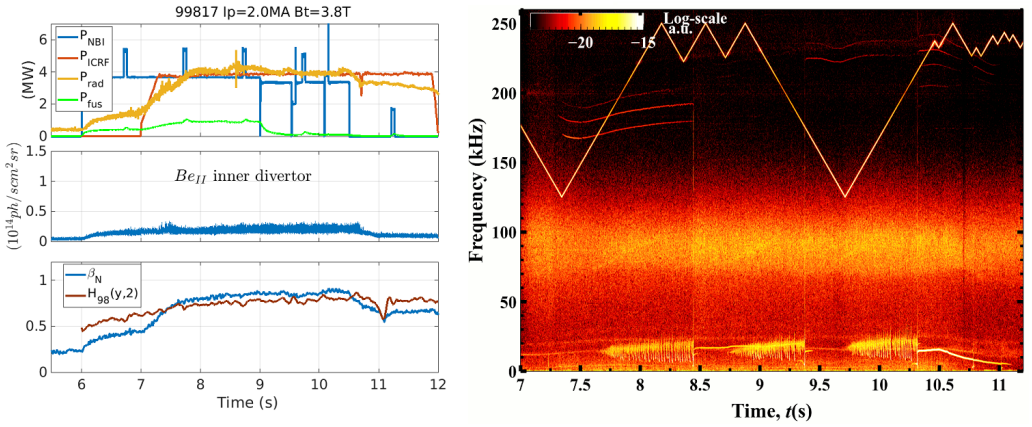

Supplementary Fig.1: Characteristics of the discharge #99817. Summary of the D-T discharge #99817 (left). Spectrogram of the discharge #99817. The AEAD signal scans frequencies ranging 100–250 kHz, with toroidal mode number spectrum $|n| < 20$ [2] (right).

in Supplementary Fig. 2. The electron temperature, T_e, obtained in these conditions reaches $T_e \sim 9.4$ keV, i.e. $T_e \sim 110$ million K, while the ion temperature reaches $T_i > 5.3$ keV or $T_i > 60$ million K, as also shown in Supplementary Fig. 2. Importantly, such temperatures are obtained with only 7.5 MW of input power. The power obtained from D-T fusion reactions is 1 MW. Strong reduction of both χ_e and χ_i, while $\chi_i/\chi_e \sim 1$ is observed in the plasma inner core at $\rho < 0.3$. The global performance of this discharge, in terms of $H_{98}(y, 2)$, is lower than #99896 due to the lower pedestal obtained at higher B_T.

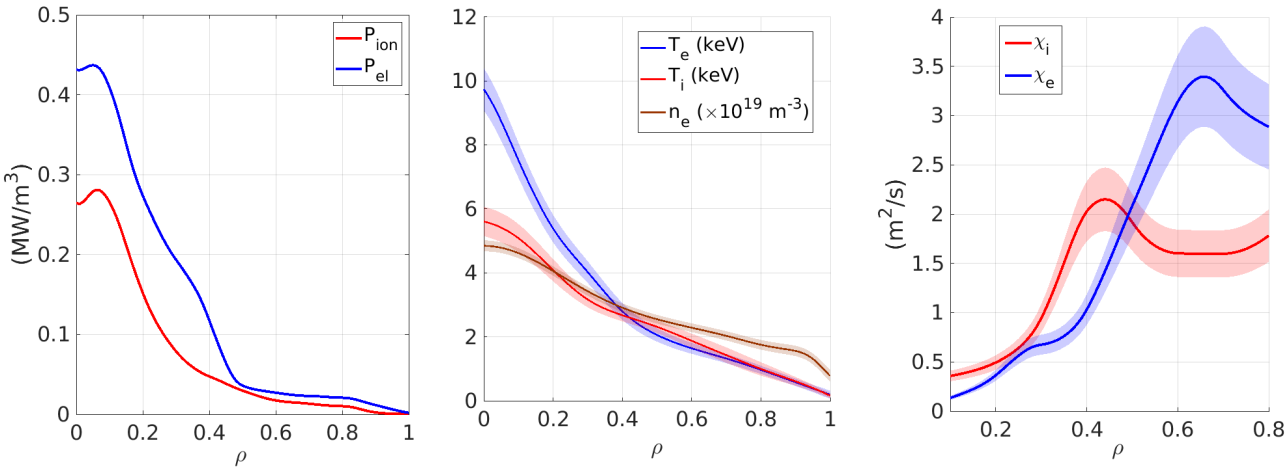

Supplementary Fig.2: Characteristics of the discharge #99817. NBI+ICRF injected power density to the electrons, P_e and ions, P_i, for the discharge #99817 at t =10 s (left). Electron, T_e and ion T_i temperature profiles and electron density, n_e, profile for the discharge #99817 at t =10 s. Shaded error bars represent standard deviation of the time-averaged signals and the systematic diagnostic uncertainties (center). χ_i and χ_e from power balance at t =10 s. Shaded error bars represent standard deviation (right).

Supplementary Note 3. D-T discharge 99896: Magnetic fluctuations analysis

The spectrogramme of magnetic fluctuations, as detected by the Mirnov coils, is shown in Supplementary Fig. 3 for the discharge #99896. The fluctuations cover frequencies from f=5 kHz to f=200 kHz. The toroidal mode number, n, is shown for each fluctuation. Both positive and negative n are detected at low and high f.

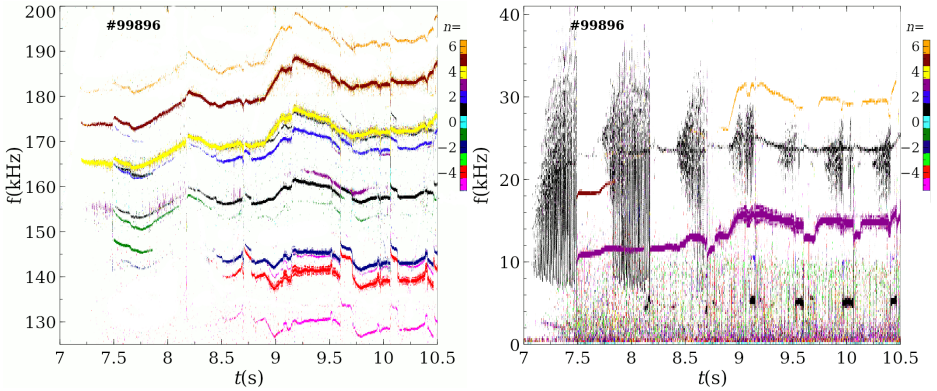

Supplementary Fig.3: Magnetic fluctuation analysis for the discharge #99896. High frequency spectrogram for the D-T discharge 99896 (left). Low frequency spectrogram for the D-T discharge 99896 (right).

Details of the bicoherence technique [3] performed to find a potential non-linear interplay between different perturbations are shown in this section. An interplay between frequencies and harmonics is identified in the TAE range and the NTM range. Such an interplay can explain the wide variety of resonances found in this discharge. For example, $f_{TAE,n=4} - f_{NTM,n=3} \approx f_{TAE,n=1} = 153$ kHz , $f_{TAE,n=5} - f_{NTM,n=3} \approx f_{TAE,n=2} = 172$ kHz. Therefore, some of the perturbations detected in this discharge are not a direct consequence of the interplay between energetic ions and Alfvén waves, but rather a non-linear interplay between different perturbations, notably TAE and NTM.

Supplementary Note 4. D-T discharge 99896: Origin of magnetic fluctuations

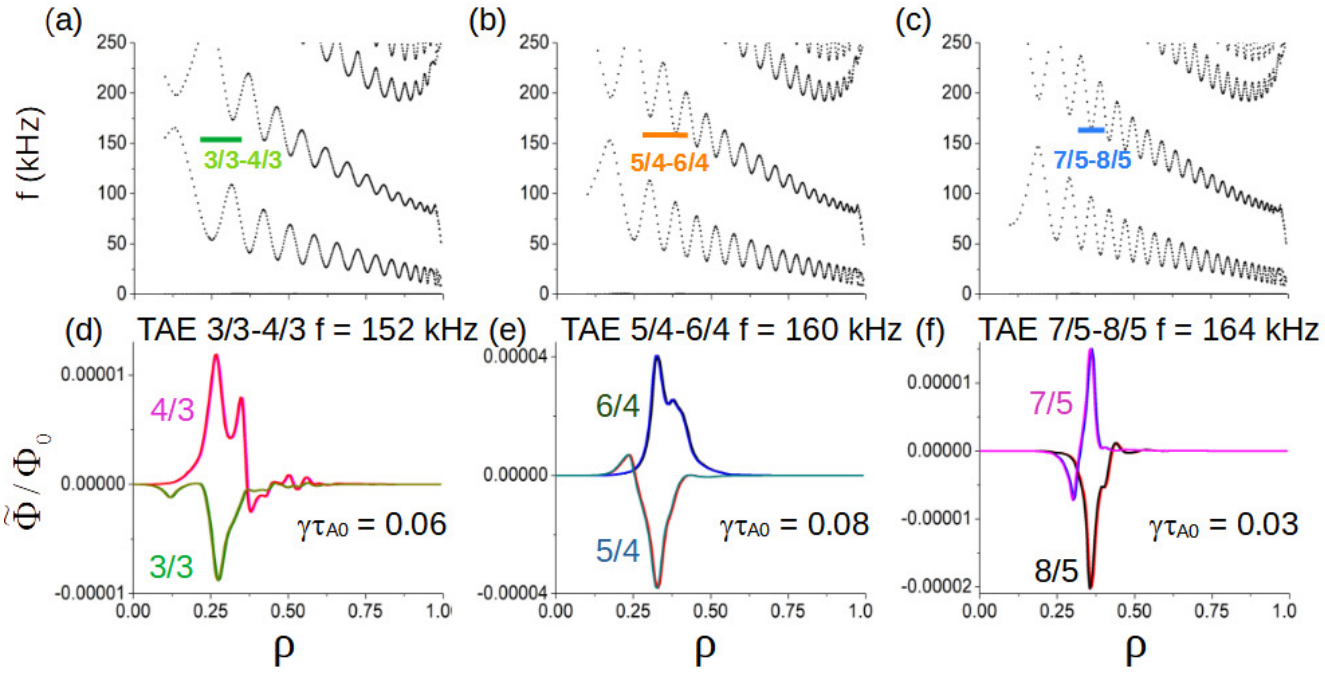

Supplementary Fig.4: FAR3D linear simulations for high frequency modes in the discharge #99896. Eingenfunctions of the electrostatic potential fluctuations, $\widetilde{\Phi}$, obtained from linear FAR3D simulations, (d),(e),(f) and comparison with the gap in the Alfvén continuum (a),(b),(c).The toroidal modes n=3,4,5 with different poloidal mode numbers are obtained. γ is the mode growth rate, τ_{A0} is the Alfvén time and $\Phi_0 = a^2 B_T/\tau_{A0}$ with a the plasma minor radius.

The origin of magnetic fluctuations has been studied by performing linear simulations with the gyrofluid code FAR3D. The energetic ions characteristics are obtained from the TRANSP code. Two energetic ion populations, H and D, are included. Electrostatic potential fluctuations with toroidal mode number n=3,4,5 are obtained in the radial location, 3.25 m $< R <$ 3.5 m and frequency, 150 kHz $< f <$ 160 kHz as shown in Supplementary Fig. 4. These results agree with the experimental data considering that the frequency in the stationary frame and the frequency in the laboratory frame are related by $f = f_{lab} - nf_{tor}$ with $f_{tor} \sim 3.34$ kHz. Such perturbations are destabilized in the gap of the Toroidal Alfvén Eingenmodes (TAE) continuum and therefore they are identified as TAE. Another perturbation with n=1 at R <3.25 m is also obtained with $f = 18$ kHz. Such a perturbation has the characteristics of the fishbone perturbation as observed in Supplementary Fig. 5.

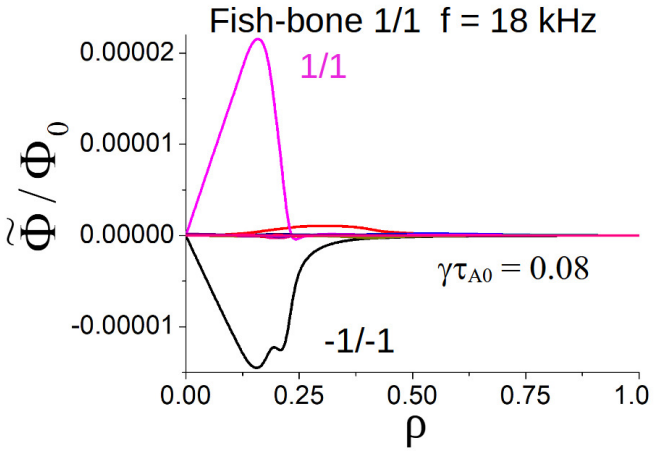

Supplementary Fig.5: FAR3D linear simulations for low frequency modes in the discharge #99896. Eingenfunction of the electrostatic potential fluctuations from linear FAR3D simulations and comparison with the gap in the Alfvén continuum.The mode n=1, identified as fishbone, is obtained.

Supplementary Note 5. Magnetic perturbation spatial location and q profile verification

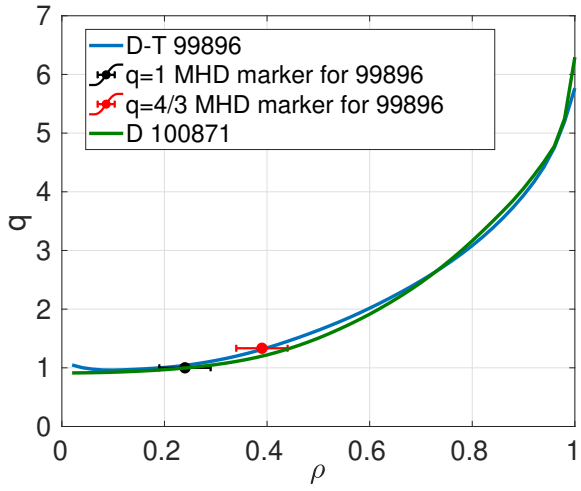

Supplementary Fig.6: Validation of the q profile used in magnetic fluctuations modelling. q profile obtained from the loop between EFIT and TRANSP for the calculation of the plasma equilibrium for D-T discharge #99896. The MHD markers corresponding to the location of q=1 (black) and q=4/3 (red) are added showing a good agreement with the derived q profile. The q profile obtained following the same procedure for the D discharge #100871 is also shown. Error bars represent uncertainties in the equilibrium reconstruction.

The validity of the q profile used in the CGYRO and FAR3D simulations for the discharge #99896 was analyzed by comparing the q profile obtained from TRANSP and the MHD markers. As depicted in Supplementary Fig. 6, the q profile obtained from TRANSP is in good agreement with the MHD markers. The q profile for the deuterium discharge #100871 is very similar to the one obtained for the discharge #99896, which means that the changes in the turbulence characteristics between both discharges cannot be a consequence of different q profile charcateritics.

Supplementary Note 6. Input Parameters used in CGYRO simulations

Supplementary Table 2: Employed plasma parameters in CGYRO simulations modelling JET pulse #99896 at $\rho = 0.31$ and $t = 8.6$ s. ϵ is the inverse aspect ratio, q the safety factor, $\hat{s}$ the magnetic shear, n the species density normalized to the electron density, $a/L_{n,T}$ the normalized logarithmic density and temperature gradient, β_e the electron-beta, ν_{ee} the electron collision rate and a the minor radius. The normalization factors in standard units are also reported, i.e. the on-axis magnetic field strength B_0, the local ($\rho = 0.31$) electron temperature T_e, density n_e and the major radius R_0.

ϵ	q	$\hat{s}$	T_i/T_e	a/L_{n_e}	a/L_{T_e}	a/L_{T_i}	n_D/n_e	n_T/n_e	a/L_{n_D}
0.30	1.17	0.74	0.76	1.00	3.20	2.40	0.58	0.39	0.93
a/L_{n_T}	n_f/n_e	T_f/T_e	β_e [%]	$\nu_{ee}a/c_s$	B_0 [T]	T_e [keV]	n_e [m^{-3}]	a [m]	R_0 [m]
0.92	0.03	21.0	0.44	0.39	2.75	3.68	$3.67 \cdot 10^{19}$	0.91	3.00

Acknowledgments

J. Garcia would like to thank Gerardo Giruzzi for fruitful discussions.

This work has been carried out within the framework of the EUROfusion Consortium, funded by the European Union via the Euratom Research and Training Programme (Grant Agreement No 101052200 — EUROfusion). Views and opinions expressed are however those of the author(s) only and do not necessarily reflect those of the European Union or the European Commission. Neither the European Union nor the European Commission can be held responsible for them.

This work was supported in part by Grants FIS2017-85252-R and PID2021-127727OB-I00 funded by the Spanish Ministry of Science, Innovation and Universities MICIU/AEI/10.13039/501100011033, by ERDF "A way of making Europe" and by ERDF/EU.

An award of computer time was provided by the INCITE program and ALCC program. This research used resources from the Oak Ridge Leadership Computing Facility, which is an Office of Science User Facility supported under Contract DE-AC05-00OR22725. Computing resources were also provided by the National Energy Research Scientific Computing Center, which is an Office of Science User Facility supported under Contract DEAC02-05CH11231.

This work was partially supported by the project US DOE under grant DE-FG02-04ER54742.

D.Z. received financial support from the AIM4EP Project (ANR-21-CE30-0018), funded by the French National Research Agency (ANR).

Author contributions

The reported experiments were devised and jointly led by Y.K., J.O., S.S., J.G. and M.B., with the key coordination of E. de la L., C.F.M and J.M. The TRANSP simulations were performed by Ž.Š. and M.P. Gyrokinetic simulations and subsequent analyses were performed by E.B, J.C. and S.M. FAR3D simulations were performed by J.V. with the assistance of D.Z. Reflectometer analyses were performed by M.D. and J.R.R. MHD analyses were performed by R.C. and M.D. Pedestal analyses were performed by E.de la L. and E.S. Alpha particle losses were investigated by P.J.B. The manuscript was written by J.G. and E. de la L. with the feedback by all the authors.

Supplementary References

[1] R.A. Tinguely, J. Gonzalez-Martin, P.G. Puglia, N. Fil, S. Dowson, M. Porkolab, I. Kumar, M. Podestà, M. Baruzzo, A. Fasoli, Ye.O. Kazakov, M.F.F. Nave, M. Nocente, J. Ongena, Ž. Štancar, and JET Contributors. Simultaneous measurements of unstable and stable alfvén eigenmodes in jet. *Nuclear Fusion*, 62(11):112008, sep 2022. doi: 10.1088/1741-4326/ac899e. URL https://dx.doi.org/10.1088/1741-4326/ac899e.

[2] P. Puglia, W. Pires de Sa, P. Blanchard, S. Dorling, S. Dowson, A. Fasoli, J. Figueiredo, R. Galvão, M. Graham, G. Jones, C. Perez von Thun, M. Porkolab, L. Ruchko, D. Testa, P. Woskov, M.A. Albarracin-Manrique, and JET Contributors. The upgraded jet toroidal alfvén eigenmode diagnostic system. *Nuclear Fusion*, 56(11): 112020, aug 2016. doi: 10.1088/0029-5515/56/11/112020. URL https://dx.doi.org/10.1088/0029-5515/56/11/112020.

[3] S. Elgar and R.T. Guza. Statistics of bicoherence. *IEEE Transactions on Acoustics, Speech, and Signal Processing*, 36(10):1667–1668, 1988. doi: 10.1109/29.7555.